Progress In Electromagnetics Research, PIER 76, 327–340, 2007

RADIATION PATTERNS SYNTHESIS FOR A CONFORMAL DIPOLE ANTENNA ARRAY

Q.-Q. He and B.-Z. Wang

Institute of Applied Physics
University of Electronic Science and Technology of China
610054, Chengdu, China

Abstract—A conformal cylindrical dipole array is developed in this paper. Because the conformal dipole array is curved, new far field pattern behaviors emerge. In this paper, we start to analyse the equations for the far field of the conformal dipole array by using the method of moments (MoM) with a dyadic Green's function, and then validate the accuracy of the far field expressions. Next, a novel Gauss amplitude distribution, which is capable to yield a desired far field radiation pattern when the array structure has a relative small cylindrical radius, is proposed. The advantage of the proposed method is that it can provide good aperture distributions to obtain low sidelobe level.

1. INTRODUCTION

The assumption of periodic identical elements in traditional linear array synthesis leads to analytical solutions that provide useful insights into array performance and behavior. But when an array is curved, some of these assumptions become invalid and linear array methods often do not apply to curved arrays. Especially for some practical applications where the placement of an element will be greatly influenced by the shape of the mounting platform, it is impossible to exploit pattern multiplication [1].

Direct analysis approaches for radiating structures mounted on arbitrarily shaped platforms are typically based on either the method of moments (MoM) [2–4], finite element methods (FEM) [5], or finite difference time domain (FDTD) techniques [6]. Furthermore, Papakanellos et al. [7] use a combined method of auxiliary sources-reaction matching approach for analyzing of arrays of arbitrarily located cylindrical dipoles. Gupta et al. [8] apply the vector potential method and fresnel-kirchhoff scalar diffraction field theory to analyze

an elliptically bent conformal array of longitudinal slots in narrow wall of rectangular waveguide. In [9], Toyama et al. analyze the characteristics of the electromagnetic scattering from periodic arrays of two-dimensional composite cylindrical objects with internal eccentric cylindrical scatterers.

The more complicated problem of synthesizing radiation patterns for arrays of conformal antennas on curved surfaces has also been studied in recent some years. Use of weighted least squares is seen in several papers where a desired pattern is used along with an iterative least squares curve-fitting procedure to select element phasing [10–12]. In [13], Bucci et al. use a projection method to select element excitations for conformal arrays by choosing only the desired patterns from a subspace of all possible radiation patterns. A simulated annealing technique previously developed for circular arc arrays is presented as a method for synthesizing the radiation pattern for three-dimensional conformal arrays in [14]. Moreover, optimization algorithms have also been widely used for different purposes in antenna array synthesis. The uses of genetic algorithm (GA) procedures to optimize array characteristics can be found in [15–18]. In [19], Boeringer et al. use a particle swarm optimization algorithm to optimize a modified Bernstein polynomial and provide a specified aperture efficiency, and family of aperture distributions and corresponding far field patterns is produced that allows aperture efficiency to be traded for sidelobe level. Similarly, the use of Bézier representations for the multiobjective optimization of conformal array amplitude weights can also be seen in [20]. Recently, Gozasht et al. [21] adapt the amplitude and phase excitation of the elements of smart antenna systems, and result in good radiation patterns. The use of directional elements in spherical array [22] for wideband synthesis is discussed, and the results show that the use of such elements can overcome the limitations of rapid variations in the amplitude of the far-field mode and enable such array to synthesize wideband patterns. In [23], the use of a new tapering window is also proposed for the uniform concentric circular arrays in order to reduce the sidelobe level at lower cost of wider beams and more practical feasibility and stability.

This paper analyzes the far field characteristics of the conformal cylindrical dipole array by using MoM with a dyadic Green's function. And then a novel conformal array synthesis method is proposed by using a Gauss amplitude distribution. Comparing with the traditional Dolph-Chebyshev and Taylor line source synthesis methods, the proposed Gauss weighting has a better ability to reduce the sidelobe level of a curved surface array. The novel method is also characterized by reduced cost and simple implementation.

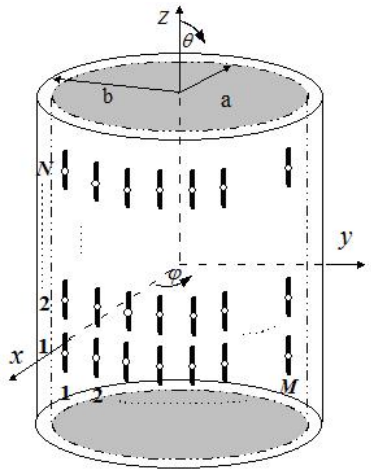

Figure 1. Geometry of a periodic cylindrical dipole array.

2. FORMULATION

Fig. 1 shows the geometry of a finite and periodic array of $N \times M$ identical dipoles mounted on the surface of a dielectric coated circular cylinder with an outer radius b, inner radius a, dielectric thickness $h = b - a$, and relative permittivity ε_r. The back of the substrate is a cylindrical perfect conductor. The circular cylinder is assumed to be infinite in the z-direction. The dipoles are oriented along the z-direction, and are assumed to be center-fed. Each dipole is assumed to have a length of $2L$, a width of W, and be uniformly spaced from its neighbors by distances of D_z in the z-direction and $D_\varphi = \Delta\varphi b$ in the φ-direction.

According to Fig. 1, the coordinate vector of the pqth element is

$$\boldsymbol{r}_{pq} = \hat{\rho}b + \hat{\varphi}\varphi_p + \hat{z}z_q \tag{1}$$

where

$$\begin{cases} \Delta\varphi = \dfrac{\varphi_0}{M-1} \\ \varphi_p = \left(p - \dfrac{M+1}{2}\right)\Delta\varphi, \quad p = 1, 2, 3, \ldots, M \\ z_q = \left(q - \dfrac{N+1}{2}\right)D_z, \quad q = 1, 2, 3, \ldots, N \end{cases} \tag{2}$$

and φ_0 is the angle subtended by the total array.

We formulate the electric field integral equation (EFIE) by enforcing the boundary condition that the total tangential electric field

must be zero on the surface of the array can be written as

$$\hat{\rho} \times [E^{inc}(\rho, \varphi, z) + E^s(\rho, \varphi, z)] = 0 \tag{3}$$

where E^{inc} is the incident field and E^s is the field due to the currents of the elements.

The boundary conditions are applied in the spatial domain and the cylindrical Fourier transform of the fields (an inverse Fourier transform in k_z and a Fourier series in φ) is defined by

$$f(\rho, \varphi, z) = \frac{1}{4\pi^2} \sum_{-\infty}^{+\infty} \int_{-\infty}^{+\infty} \tilde{f}(\rho, n, k_z) e^{-jn\varphi} e^{-jk_z z} dk_z \tag{4}$$

where $\tilde{f}(\rho, n, k_z)$ is the Fourier transform of $f(\rho, \varphi, z)$.

According to [24], the dipoles are assumed to be thin ($W \ll L$), so only z-directed currents exist. Thus, there is no current component in the ρ-direction. Using the proper Green's function of the structure, the field produced by the currents of the elements can be written as

$$\begin{aligned} \boldsymbol{E}^s(\varphi, z) \;=\; & \frac{1}{4\pi^2} \sum_{p=1}^{M} \sum_{q=1}^{N} \int_{-\infty}^{+\infty} \sum_{n=-\infty}^{+\infty} \tilde{\boldsymbol{G}}(n, k_z) \\ & \cdot \tilde{\boldsymbol{I}}_{pq}(n, k_z) e^{-jn(\varphi - \varphi_p)} e^{-jk_z(z - z_q)} dk_z \end{aligned} \tag{5}$$

where $\tilde{\boldsymbol{G}}(n, k_z)$ is the dyadic Green's function in the spectral domain for the electric field and $\tilde{\boldsymbol{I}}_{pq}(n, k_z)$ is the Fourier transform of the pqth element currents. The dyadic Green's function $\tilde{\boldsymbol{G}}(n, k_z)$ in equation (5) is given explicitly by [25] as

$$\tilde{G}(n, k_z) = \frac{jZ_0}{k_0} \left(k_0^2 - k_z^2\right) \frac{T_1}{T_1 T_2 - T_3^2} \tag{6}$$

where

$$T_1 \;=\; \sqrt{k_0^2 - k_z^2} \frac{H_n^{(2)'}\left(\sqrt{k_0^2 - k_z^2} b\right)}{H_n^{(2)}\left(\sqrt{k_0^2 - k_z^2} b\right)} - \frac{k_0^2 - k_z^2}{\varepsilon_r k_0^2 - k_z^2} C_1 \tag{7a}$$

$$T_2 \;=\; \sqrt{k_0^2 - k_z^2} \frac{H_n^{(2)'}\left(\sqrt{k_0^2 - k_z^2} b\right)}{H_n^{(2)}\left(\sqrt{k_0^2 - k_z^2} b\right)} - \frac{\varepsilon_r \left(k_0^2 - k_z^2\right)}{\varepsilon_r k_0^2 - k_z^2} C_2 \tag{7b}$$

$$T_3 \;=\; \frac{k_0(\varepsilon_r - 1)}{\varepsilon_r k_0^2 - k_z^2} \frac{n k_z}{b} \tag{7c}$$

and

$$C_1 = \sqrt{\varepsilon_r k_0^2 - k_z^2} \frac{\begin{pmatrix} J_n'\left(\sqrt{\varepsilon_r k_0^2 - k_z^2}a\right) N_n'\left(\sqrt{\varepsilon_r k_0^2 - k_z^2}b\right) \\ -J_n'\left(\sqrt{\varepsilon_r k_0^2 - k_z^2}b\right) N_n'\left(\sqrt{\varepsilon_r k_0^2 - k_z^2}a\right) \end{pmatrix}}{\begin{pmatrix} J_n'\left(\sqrt{\varepsilon_r k_0^2 - k_z^2}a\right) N_n\left(\sqrt{\varepsilon_r k_0^2 - k_z^2}b\right) \\ -J_n\left(\sqrt{\varepsilon_r k_0^2 - k_z^2}b\right) N_n'\left(\sqrt{\varepsilon_r k_0^2 - k_z^2}a\right) \end{pmatrix}} \tag{8a}$$

$$C_2 = \sqrt{\varepsilon_r k_0^2 - k_z^2} \frac{\begin{pmatrix} J_n\left(\sqrt{\varepsilon_r k_0^2 - k_z^2}a\right) N_n'\left(\sqrt{\varepsilon_r k_0^2 - k_z^2}b\right) \\ -J_n'\left(\sqrt{\varepsilon_r k_0^2 - k_z^2}b\right) N_n\left(\sqrt{\varepsilon_r k_0^2 - k_z^2}a\right) \end{pmatrix}}{\begin{pmatrix} J_n'\left(\sqrt{\varepsilon_r k_0^2 - k_z^2}a\right) N_n\left(\sqrt{\varepsilon_r k_0^2 - k_z^2}b\right) \\ -J_n\left(\sqrt{\varepsilon_r k_0^2 - k_z^2}b\right) N_n\left(\sqrt{\varepsilon_r k_0^2 - k_z^2}a\right) \end{pmatrix}} \tag{8b}$$

where k_0 is the free-space wave number, Z_0 is the free space intrinsic impedance, and $(')$ denotes derivative with respect to the argument.

Since the printed dipole is regarded as infinitely thin, the surface current distribution on the pqth element can be given as

$$I_{pq}(\varphi', z') = \sum_{i=1}^{N_D - 1} I_{pqi} S_{pqi}(z') \tag{9}$$

where I_{pqi} is the unknown coefficient that determines the total current at the feed point on the pqth element, $S_{pqi}(\varphi', z')$ is the piecewise sinusoidal (PWS) basis function, defined as

$$S_{pqi}(\varphi', z') = \hat{z} \begin{cases} \dfrac{\sin k_e(L - |z' - z_i|)}{\sin(k_e L)}, & z_{i-1} \le z' \le z_{i+1} \\ 0, & \text{otherwise} \end{cases} \tag{10}$$

where k_e is the wave number of the expansion mode, chosen here as

$$k_e = k_0 \sqrt{(\varepsilon_r + 1)/2} \tag{11}$$

Galerkin's method is used to form a MoM solution wherein the integral equation is discretized into a system of linear equations to be solved for the unknown coefficients I_{pqi}. Testing this equation by the same

set of basis functions (testing functions), denoted by $W_{stj}(\varphi, z)$ ($j = 1, 2, 3, \ldots, N_D$), the following matrix equation is obtained as

$$[\boldsymbol{Z}]\boldsymbol{I} = \boldsymbol{V} \tag{12}$$

where

$$Z_{pq,st} = \frac{1}{(2\pi)^2} \sum_{p=1}^{M} \sum_{q=1}^{N} \sum_{n=-\infty}^{+\infty} \int_{-\infty}^{+\infty} \tilde{W}_{st}(-n,-k_z)\tilde{\boldsymbol{G}}(n,k_z)\cdot\tilde{\boldsymbol{I}}_{pq}(n,k_z)dk_z \tag{13}$$

$$\boldsymbol{I} = [I_{pq1}, I_{pq2}, I_{pq3}, \ldots, I_{pqN_D}]^T \tag{14}$$

$$V_{stj} = -\iint_{S_{stj}} dsW_{stj}(\rho,\varphi,z)\cdot\hat{n}\times E^{inc}(\rho,\varphi,z) \tag{15}$$

The most crucial problem is how to solve the integral in equation (13). According to [26], the integration alone the k_z axis is deformed as shown in Fig. 2 to avoid the poles of the integrand between $k_z = k_0$ and $k_z = \sqrt{\varepsilon_r}k_0$. The integration contour can be chosen more or less arbitrarily, but it is not advisable to get too far from the real axis to avoid numerical problems. In this paper, we have chosen a distance of $0.1k_0$ from the real axis. Simultaneously, the expressions for the electromagnetic field, in the spectral domain, due to a current on a cylinder, contain Bessel and Hankel functions. To improve the numerical efficiency we tabulate their values for the arguments needed, i.e., for each k_z we make a table of the values of the Bessel and Hankel functions for all order and arguments. For large order Bessel and Hankel functions we use Debye's asymptotic formulas to deal with the integral. The Debye's asymptotic formulas can be obtained as follows [27]

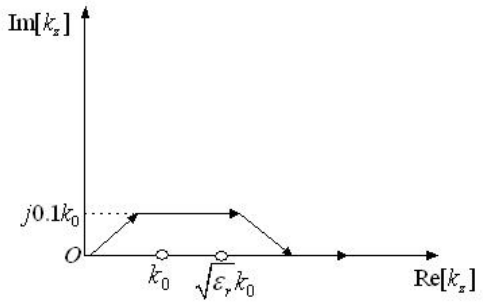

Figure 2. Deformation of the integration path in a complex integration contour.

$$J_n(x) \cong \frac{e^{-n\left[\frac{n}{x}-\tanh\left(\frac{n}{x}\right)\right]}}{\sqrt{2\pi n \tanh\left(\frac{n}{x}\right)}} \left\{1+\frac{3\coth\left(\frac{n}{x}\right)-5\left[\coth\left(\frac{n}{x}\right)\right]^3}{24n}\right\} \quad (16a)$$

$$H_n^{(2)}(x) \cong j\frac{e^{n\left[\frac{n}{x}-\tanh\left(\frac{n}{x}\right)\right]}}{\sqrt{0.5\pi n \tanh\left(\frac{n}{x}\right)}} \left\{1-\frac{3\coth\left(\frac{n}{x}\right)-5\left[\coth\left(\frac{n}{x}\right)\right]^3}{24n}\right\} \quad (16b)$$

In (16), the condition for order n of Bessel and Hankel functions is $|n-x| \geq |x|^{1/3}$ for all used arguments x during the integration procedure [27].

Next, the radiation field of the pqth element can be calculated in the following way [28]

$$\begin{aligned}\tilde{E}_{zpq}(n,k_z,\rho) &= \tilde{E}_{zpq}(n,k_z,b)\cdot\frac{H_n^{(2)}(k_\rho\rho)}{H_n^{(2)}(k_\rho b)} \\ &= \left[\int_{-\infty}^{+\infty}\sum_{n=-\infty}^{+\infty}\boldsymbol{G}(b,\varphi,z)\cdot\boldsymbol{I}_{pq}(b,\varphi,z)e^{jn(\varphi-\varphi_p)}e^{jk_z(z-z_q)}dk_z\right] \\ &\quad\cdot\frac{H_n^{(2)}(k_\rho\rho)}{H_n^{(2)}(k_\rho b)} \end{aligned} \quad (17)$$

where the ρ is the far field radius and $H_n^{(2)}$ is the Hankel function of second kind that describes an outward traveling in the far field. In order to obtain the E_z field component in the spatial domain, we need to evaluate the k_z integral in (4). This is made in approximate way using the stationary phase method [29] (notice that the phase is fastly changing due the term $H_n^{(2)}(k_\rho\rho)e^{-jk_zz}$). The resulting expression for E_z field component in far field is

$$\begin{aligned}E_z(\rho,\theta,\varphi) &= \sum_{p=1}^{M}\sum_{q=1}^{N}E_{zpq}(\rho,\theta,\varphi) \\ &= \frac{j}{\pi}\sum_{p=1}^{M}\sum_{q=1}^{N}\sum_{n=-\infty}^{+\infty}j^n e^{-jn\varphi}\frac{\tilde{E}_z(n,k_0,\cos\theta,b)}{H_n^{(2)}(k_0\sin\theta b)}\frac{e^{-jkr}}{r}\end{aligned} \quad (18)$$

In order to validate the accuracy of the far field expressions by using our method, we calculate the cylindrical array of thin printed dipoles in literature [3]. The comparing results are shown in Fig. 3 and a good agreement is obtained.

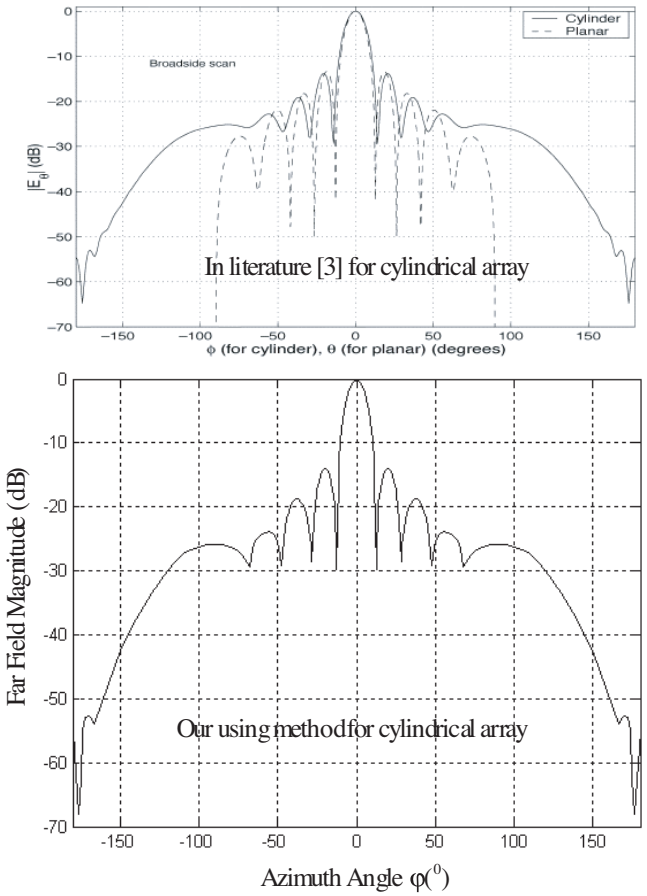

Figure 3. The result comparison based on literature [3] and our using method.

3. RADIATION PATTERNS SYNTHESIS

In this paper, a 10×12 printed dipole array, with an outer radius of circular cylinder $b = 9\lambda_0$, dielectric thickness $h = 0.25\lambda_0$, and relative permittivity $\varepsilon_r = 2.1$, is designed, where λ_0 is the free space wavelength corresponding to an operating frequency of 10 GHz. The dipoles ($2L = 0.5\lambda_0$, $W = 0.003\lambda_0$) are mounted on the surface of the circular cylinder within the range of $|\varphi_0| \leq 60^\circ$ and the spaces between neighbors are $0.86\lambda_0$ and $0.856\lambda_0$ in the z-direction and φ-direction, respectively. According to the coordinate relations of the

array elements created in Fig. 1, φ is called azimuth angle and θ is called elevation angle. Since the cylindrical dipole array has a perfect ground and placed on the surface of the circular cylinder within the range of $|\varphi_0| \leq 60^\circ$, the azimuth scope of the far field is mainly in the range of $\varphi = -\pi/2 \sim \pi/2$. In the back of the dipole array, the radiation may be neglected. Similarly, the azimuth scope of the far field is mainly in the range of $\theta = 0 \sim \pi$.

Fig. 4 presents the far field patterns for the cylindrical array when each dipole is excited uniformly and has an identical phase. From Fig. 4, we can see that the effect of the structure curvature on the cylindrical array properties is very big in the azimuth plane (φ). The mianbeam can not be shaped when the cylinder has a relative small cylindrical radius. In the elevation plane (θ), the effect of the structure curvature on the array properties is small.

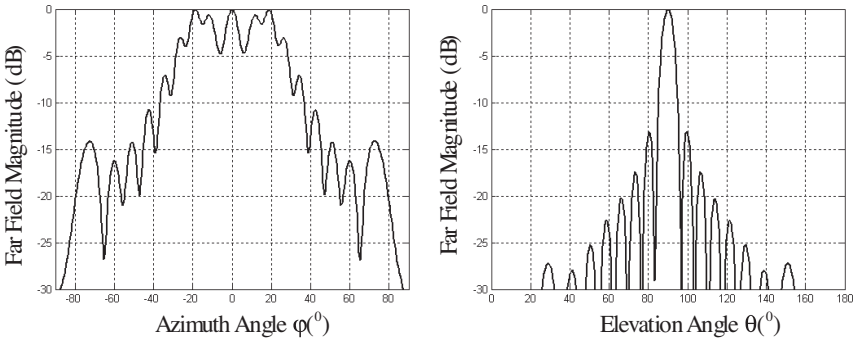

Figure 4. The far field patterns based on equal amplitude and identical phase excited.

However, for certain purposes the patterns of arrays are usually designed to have narrow mainbeam and low sidelobe levels (SLLs). These designs are often based on either the Dolph-Chebyshev or the Taylor line source methods that work well in general but are not optimized for any applications. Especially for many practical applications where the place of an element will be greatly influenced by the shape of the mounting platform, the uses of the Dolph-Chebyshev and Taylor line source methods are no longer possible to obtain low SLLs.

Fig. 5 gives the far field patterns by using the Dolph-Chebyshev and Taylor line source methods, respectively. It is shown that two conventional methods give about consistent results and a 30 dB Taylor or Chebyshev weighting only obtains about 1.9 dB SLLs in the azimuth

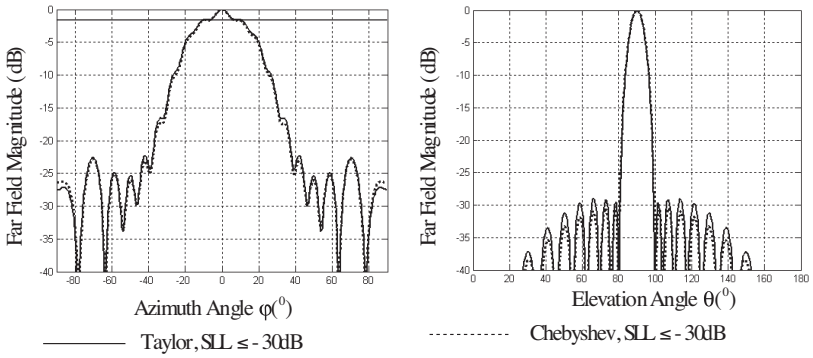

Figure 5. The far field patterns based on Chebyshev and the Taylor line source methods.

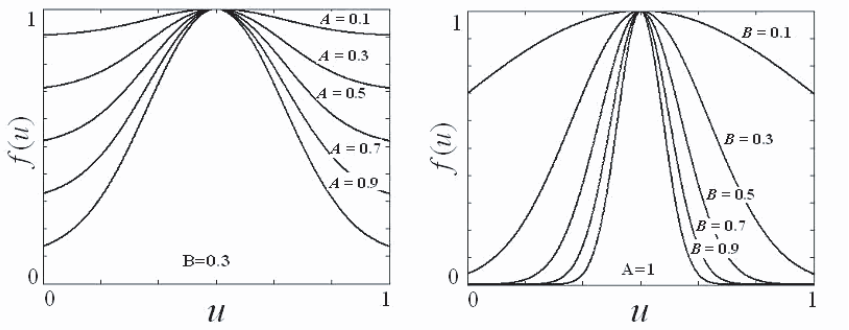

Figure 6. The Gauss curves based on selecting different A and B.

plane. Away from the main lobe, the shapes of the patterns change significantly. High sidelobes occur unregularly because of the effect of curvature of the cylinder. Therefore, the port excitations must be modified for the cylindrical array to avoid these high sidelobes. In fact, array synthesis algorithms for the cylindrical array have to be different from the well known algorithms for the planar case.

Thus, novel cylindrical array amplitude weights must be taken into account. The Gauss expression provides a flexible method for specifying smooth unimodal functions, which are typically expected and desired for linear and cylindrical array aperture amplitude weights. It is defined with two parameters A and B as

$$f(u) = -A\left[1 - e^{-(Bu)^2}\right] + 1 \tag{19}$$

Fig. 6 shows the Gauss curves based on different A and B. Selecting different A and B, we can obtian different aperture distributions. Fig. 7

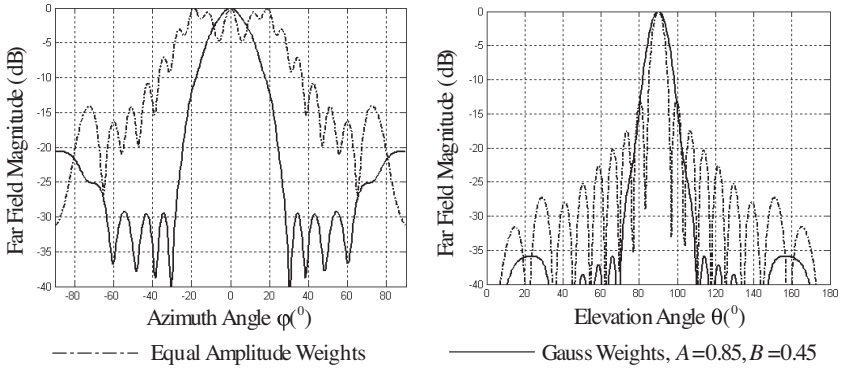

Figure 7. The far field patterns based on Gauss amplitude distributions.

gives the far field patterns of the cylindrical dipole array by using the Gauss curve as excitation amplitude weights. It is shown that a good mainbeam can be shaped with a 20 dB SLL in the azimuth plane, while away from the main lobe, high sidelobes still occur unregularly owing to inherence property of cylinder. In the elevation plane, the use of Gauss weights may obtian a 35 dB SLL, and the effect of the structure curvature on far field properties is slender. Compared with the results in Fig. 5 given by the Taylor and Chebyshev distributions, better radiation patterns have been obtained with the Gauss amplitude distribution.

4. CONCLUSIONS

In this paper, we analyze the far field characteristics of the cylindrical dipole array by using MoM with a dyadic Green's function. Next, we synthetize far field patterns with a 20 dB SLL in the azimuth plane and a 35 dB SLL in the elevation plane by using this proposed novel method. Thus, the novel synthesis method can produce a good performance, effectively reduce SLLs when the conventional Dolph-Chebyshev and Taylor line source synthesis methods is limited to do so.

However, we can also find that the inherence curvature trait of cylindrical structure, or some complicated conformal curved surface, will lead to the radating directions of array elements becoming unconsistent. Thus, away from the mainbeam, high sidelobes still occur when the novel synthesis method is used. One possible approach for solving this generalized synthesis problem is through the use of

pattern reconfigurable elements. Because reconfigurable element can radiate with more than one element pattern, the technique can let the patterns of conformal array elements become similar and identical, and overcome the structure curvature influence in certain extent.

ACKNOWLEDGMENT

This work was supported by the National Natural Science Foundation of China (No.90505001), the High-Tech Research and Development Program of China (No. 2006AA01Z275), and the Creative Research Group Program of UESTC,

REFERENCES

1. Kumar, W., "Preface," *IEEE Transctions on Antennas and Propagation*, Vol. AP-22, No. 1, 1–3, Jan. 1974.
2. Raffaelli, S., "Analysis and measurements of conformal patch array antennas on multiplayer circular cylinder," *IEEE Transctions on Antennas and Propagation*, Vol. 53, No. 3, 1105–1113, Mar. 2005.
3. Erturk, V. B., R. G. Rojas, and K. W. Lee, "Analysis of finite arrays of axially directed printed dipoles on electrically large circular cylinders," *IEEE Transctions on Antennas and Propagation*, Vol. 52, No. 10, 2586–2595, Oct. 2004.
4. Liu, Z.-F., P.-S. Kooi, L.-W. Li, M.-S. Leong, and T.-S. Yeo, "A method of moments analysis of a microstrip phased array in three-layered structures," *Progress In Electromagnetics Research*, PIER 31, 155–179, 2001.
5. Macon, C. A., L. C. Kempel, S. W. Schneider, and K. D. Trott, "Modeling conformal antennas on metallic prolate spheroid surfaces using a hybrid finite element method," *IEEE Transctions on Antennas and Propagation*, Vol. 52, No. 3, 750–758, Mar. 2004.
6. Yu, W., Y. Liu, T. Su, N.-T. Huang, and R. Mittra, "A robust parallel conformal FDTD algorithm and its application to electrically large antenna array simulation," *IEEE 2004 Antenna Propagat. Symp.*, Vol. 1, 1030–1033, Jun. 2004.
7. Papakanellos, P. I., I. I. Heretakis, and P. K. Varlamos, "A combined method of auxiliary soures-reaction matching approach for analyzing moderately large-scale arrays of cylindrical dipoles," *Progress In Electromagnetics Research*, PIER 59, 51–67, 2006.
8. Gupta, R. C. and S. P. Singh, "Elliptically bent slotted waveguide conformal focused array for hyperthermia treatment of tumors

in curved region of human body," *Progress In Electromagnetics Research*, PIER 62, 107–125, 2006.

9. Toyama, H. and K. Yasumoto, "Electromagnetic scattering from periodic arrays of composite circular cylinder with internal cylindrical scatterers," *Progress In Electromagnetics Research*, PIER 52, 321–333, 2005.
10. Athanasopoulos, N. C. and N. K. Uzunoglu, "Development of a phased array full duplex-conformal 10 GHz antenna system incorporating radiation pattern optimization algorithms," *Radar Conference, European*, 307–310, Oct. 2005.
11. Vaskelainen, L. I., "Iterative least-squares synthesis methods for conformal array antennas with optimized polarization and frequency properties," *IEEE Transctions on Antennas and Propagation*, Vol. 45, No. 7, 1179–1185, July 1997.
12. Athanasopoulos, N. C., N. K. Uzunoglu, and J. D. Kanellopoulos, "Development of a 10 GHz phased array cylindrical antenna system in corporating IF phase processing," *Progress In Electromagnetics Research*, PIER 59, 17–38, 2006.
13. Bucci, O. M., G. D'Elia, and G. Romito, "Power synthesis of conformal arrays by a generalized projection method," *IEE Proc. - Microw. Antennas and Propag.*, Vol. 142, No. 6, 467–471, Dec. 1995.
14. Ferreira, J. A. and F. Ares, "Pattern synthesis of conformal arrays by the simulated annealing technique," *Electronic Letters*, Vol. 33, No. 14, 1187–1189, July 1997.
15. Yan, K.-K. and Y. Lu, "Sidelobe reduction in array-pattern synthesis using genetic algorithms," *IEEE Transctions on Antennas and Propagation*, Vol. 45, 1117–1122, July 1997.
16. Allard, R. J., D. H. Werner, and P. L. Werner, "Radiation pattern synthesis for arrays of conformal antennas mounted on arbitrarily-shaped three-dimensional platforms using genetic algorithms," *IEEE Transctions on Antennas and Propagation*, Vol. 51, No. 5, 1054–1062, May 2003.
17. Mitilineos, S. A., S. C. A. Thomopoulos, and C. N. Capsalis, "Genetic design of dual-band, switched-beam dipole arrays, with elements failure correction, retaining constant excitation coefficients," *Journal of Electromagnetic Waves and Applications*, Vol. 20, No. 14, 1925–1942, 2006.
18. Ayestarán, R. G., J. Laviada, and F. Las-Heras, "Synthesis of passive-dipole arrays with a genetic-neural hybrid method," *Journal of Electromagnetic Waves and Applications*, Vol. 20, No. 15, 2123–2135, 2006.

19. Boeringer, D. W. and D. H. Werner, "Efficiency-constrained particle swarm optimization of a modified Bernstain polynomial for conformal array excitation amplitude synthesis," *IEEE Transctions on Antennas and Propagation*, Vol. 53, No. 8, 2662–2673, Aug. 2005.
20. Boeringer, D. W. and D. H. Werner, "Bézier representations for the multiobjective optimization of conformal array amplitude weights," *IEEE Transctions on Antennas and Propagation*, Vol. 54, No. 7, 1964–1970, July 2006.
21. Gozasht, F., G. Dadashzadeh, and S. Nikmhr, "A comprehensive performance study of circular and hexagonal array geometries in the LMS algorithm for smart antenna applications," *Progress In Electromagnetics Research*, PIER 68, 281–296, 2007.
22. Huang, M. D. and S. Y. Tan, "An improved spherical antenna array for wideband phase mode processing," *Progress In Electromagnetics Research*, PIER 59, 17–38, 2006.
23. Dessouky, M., H. Sharshar, and Y. Albagory, "A novel tapered beamforming window for uniform concentric circular arrays," *Journal of Electromagnetic Waves and Applications*, Vol. 20, No. 14, 2077–2089, 2006.
24. Pozar, D. M., "Analysis of finite phased arrays of printed dipoles," *IEEE Transctions on Antennas and Propagation*, Vol. AP-33, No. 10, 1045–1053, Oct. 1985.
25. Nakatini, A., N. G. Alezopoulos, N. K. Uzunoglu, and P. L. E. Uslenghi, "Accurate Green's function computation for printed circuit antennas on cylindrical antennas," *Electromagnetics*, Vol. 6, 243–254, July–Sept. 1986.
26. Rana, I. E. and N. G. Alezopoulos, "Current distribution and input impedance of printed dipole," *IEEE Transctions on Antennas and Propagation*, Vol. AP-29, No. 1, 933–946, Jan. 1981.
27. Naishadham, K. and L. Felsen, "Dispersion of waves guided along a cylindrical substrate-superstrate layered medium," *IEEE Transctions on Antennas and Propagation*, Vol. 41, No. 3, 304–313, Mar. 1993.
28. Habashy, T. M., S. M. Ali, and J. A. Kong, "Input impedance and radiation pattern of cylindrical-rectangular and wraparound microstrip antennas," *IEEE Transctions on Antennas and Propagation*, Vol. AP-38, No. 5, 722–731, May 1990.
29. Ashkenazy, J., S. Shtrikman, and D. Treves, "Electric surface current model for the analysis of microstrip antennas on cylindrical bodies," *IEEE Transctions on Antennas and Propagation*, Vol. AP-33, No. 3, 295–300, Mar. 1985.